

# Chain-Folded Lamellar Structure in the Smectic H Phase of a Main-Chain Polyester

Masatoshi Tokita,<sup>†</sup> Kensuke Osada, Masayuki Yamada, and Junji Watanabe\*

Department of Polymer Chemistry, Tokyo Institute of Technology, Ookayama, Meguro-ku, Tokyo 152, Japan

Received June 29, 1998

**ABSTRACT:** Smectic state morphology of the main-chain liquid crystal PB-14 polyester was studied by small-angle X-ray scattering (SAXS), differential scanning calorimetry, and transmission electron microscope methods. The PB-14 polyester forms isotropic liquid (I), smectic H ( $S_H$ ), and crystalline phases in order of decreasing temperature. The transition temperature between the I and  $S_H$  phases was 226 °C on heating and 210 °C on cooling when it was measured at a rate of 10 °C min<sup>-1</sup>. SAXS for the  $S_H$  phase formed from the isotropic melt showed well-defined reflection maxima which are attributed to the chain-folded lamellar structure. The lamellar size increased from 300 Å to 500 Å with an increase of the liquid crystallization temperature of 190 °C to 220 °C. The relationship between the lamellar thickness and isotropization temperature is well described by the Thomson–Gibbs equation. According to this relationship, the surface free energy of the lamellae and the equilibrium isotropization temperature of  $S_H$  were elucidated as 72 erg cm<sup>-2</sup> and 263 °C, respectively. When the sample was annealed at a  $S_H$  temperature of 215 °C, the isotropization temperature of the  $S_H$  phase increased from 228 °C to 257 °C, and simultaneously the enthalpy change increased from 4.9 kcal mol<sup>-1</sup> to 6.0 kcal mol<sup>-1</sup>. These trends can be explained by the lamellar thickening. The overall results thus indicate that the  $S_H$  liquid crystallization at a certain temperature takes place imperfectly in a finite period due to the chain folding and that the succeeding annealing causes the alteration of the chain conformation from a folded form to an extended one as observed in the crystallization of conventional polymers.

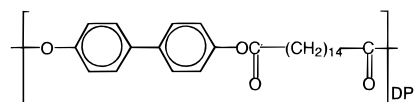
## 1. Introduction

Semiflexible homopolymers having rigid aromatic and flexible alkylene segments in a repeating unit are an attractive object of investigation because they form liquid crystalline phases. The polymers are termed main-chain liquid crystalline (LC) polymers. Appearance of a mesophase is a consequence of the existence of an anisotropic intermolecular interaction associated with the anisotropic shape of molecules. The chain backbone thus can be assumed to take an extended configuration at least in a local space of the LC field.<sup>1</sup>

Here, the question arises as to whether the polymer chains are extended or not along the entire length.<sup>1–5</sup> As the first challenge to answer this question, we studied the solid-state morphology of the main-chain LC poly(hexamethylene bibenzoate) (BB-6) by the small-angle X-ray scattering (SAXS) method.<sup>6,7</sup> The BB-6 polyester forms isotropic, smectic A ( $S_A$ ), and crystal phases in order of decreasing temperature, its crystallization thereby taking place from the  $S_A$  phase. SAXS for the crystalline specimens, which were prepared by cooling the isotropic melt at a rate of 10 °C min<sup>-1</sup>, showed well-defined reflection maxima which were attributed to the stacked lamellar structure. The lamellar spacings were distributed around 250 Å so that an appreciable number of chain foldings were included in a chain. For the film sample which was prepared by applying shear flow in the smectic state, the reflection spots appeared perpendicularly to the shear direction, showing that the shear flow arranged the lamellae parallel to its direction.<sup>6,8,9</sup> This anomalous orientation

strongly suggests that the chain folded lamellar structure already exists in the foregoing smectic state, although no SAXS maximum is observed in the smectic state.

In this study, we performed SAXS measurements for another type of smectic phase, namely the smectic H ( $S_H$ ) phase, formed by the following main-chain PB-14 polymer,<sup>10–14</sup>



and observed the well-defined reflections attributable to the lamellar structure. We will describe the liquid crystal morphology in detail according to this observation.

## 2. Experimental Section

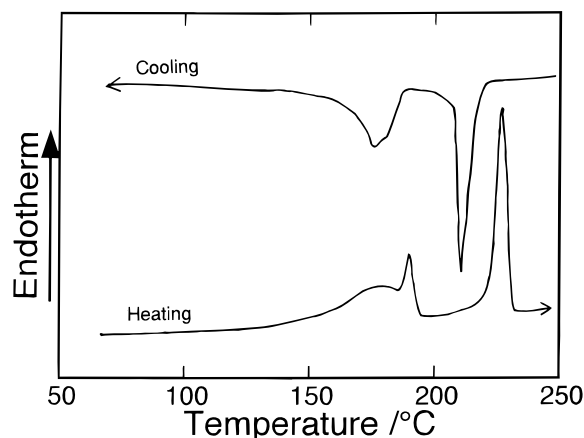
The PB-14 polyesters were prepared by melt condensation of 4,4'-diacetoxybiphenyl and tetradecanedioic acids. Two specimens with different molecular weights, PB-14-I and PB-14-II, were prepared by controlling the reaction period of melt transesterification (see Table 1). Inherent viscosities of the samples were determined at 30 °C using a 0.5 g dL<sup>-1</sup> solution in a 60/40 mixture by weight of phenol and tetrachloroethane. The calorimetric behavior was investigated with a Perkin-Elmer DSC-II calorimeter under a flow of dry nitrogen. Wide-angle X-ray (WAXS) and SAXS measurements were performed using a Rigaku-Denki X-ray generator with Ni-filtered CuK $\alpha$  radiation and a flat imaging plate. The sample temperature was measured and regulated with an accuracy of 0.2 °C by using a Mettler FP-80 hot stage. The lamellar spacing from the SAXS measurement was evaluated with a possible error of  $\pm 5$  Å. Transmission electron microscope (TEM) observation to clarify the morphology of the polymer was performed by a Hitachi H-500 TEM with 100 kV of accelerating voltage. For

<sup>†</sup> Present address: Graduate School of Bio-Applications and Systems Engineering, Tokyo University of Agriculture and Technology, Koganei, Tokyo 184, Japan.

\* Corresponding author.

**Table 1. Characterization of PB-14 Polyesters**

| sample   | $\eta_{inh}$<br>(dL g <sup>-1</sup> ) | calorimetric data       |       |       |                         |       |       |     | transition<br>enthalpy <sup>a</sup><br>(kcal mol <sup>-1</sup> ) |  |
|----------|---------------------------------------|-------------------------|-------|-------|-------------------------|-------|-------|-----|--|--|
|          |                                       | heating<br>process (°C) |       |       | cooling<br>process (°C) |       |       |     | $\Delta H_1 + \Delta H_2$  |  |
|          |                                       | $T_1$                   | $T_2$ | $T_i$ | $T_1$                   | $T_2$ | $T_i$ |     |  |  |
|          |                                       |                         |       |       |                         |       |       |     |  |  |
| PB-14-I  | 0.76                                  | 181                     | 191   | 226   | 173                     | 178   | 210   | 4.9 | 5.2  |  |
| PB-14-II | 1.17                                  | 180                     | 191   | 228   | 173                     | 178   | 210   | 4.9 | 5.1  |  |

<sup>a</sup> Based on cooling DSC data.**Figure 1.** Heating and cooling DSC thermograms of PB-14-I measured at a scanning rate of 10 °C min<sup>-1</sup>.

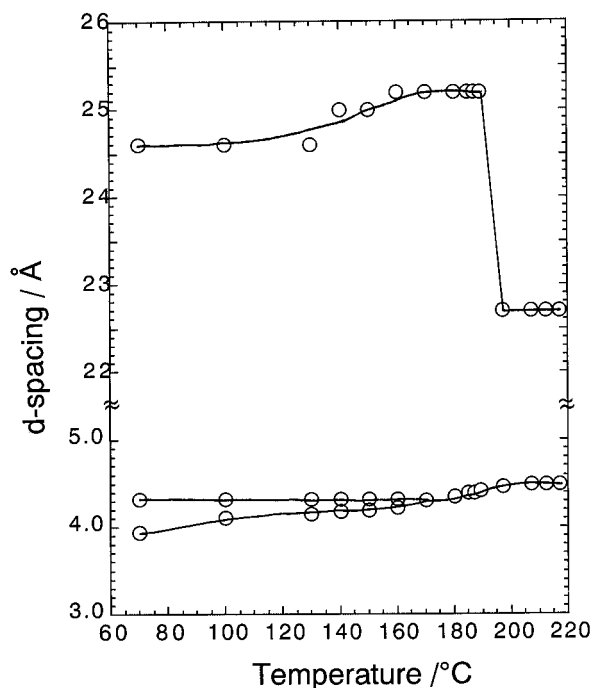
this observation, an ultrathin section of the polymer was prepared as follows. The bulk polymer was cut into ultrathin sections (700 Å thick) by an ultramicrotome with a diamond knife. The sectioned specimen was stained with the vapor of RuO<sub>4</sub> for 10 min before observation.

### 3. Results and Discussion

**3.1. Characterization of Polymers.** Figure 1 shows the differential scanning calorimetry (DSC) thermogram of PB-14-I. The DSC thermogram includes two sharp peaks and one broad peak in both the heating and cooling curves. The two sharp peaks on heating indicate a  $K_2 - S_H$  transition and isotropization of the  $S_H$  phase, respectively.<sup>12,14</sup> The additional broad peak at a temperature just below the  $K_2 - S_H$  transition shows a crystal-crystal transition,  $K_1 - K_2$ .<sup>12, 14</sup>

These transitions have also been followed by the change in the  $d$  spacings of the X-ray reflections as illustrated in Figure 2. With an increase of temperature in the crystalline region, the spacing of the inner layer reflection increased from 24.6 to 25.2 Å and the two outer reflections merged with each other. At the  $K_2 - S_H$  transition at 191 °C, the layer spacing of 25.2 Å drops suddenly to 22.7 Å. Although an oriented sample was not obtainable, the reflection spacings indicate that the molecules in the  $S_H$  phase are packed into a two-dimensional orthogonal unit-cell where  $a' = 9.0$  Å;  $b' = 6.1$  Å; and  $\gamma' = 90^\circ$ .<sup>10,11</sup> The layer spacing of 22.7 Å is appreciably smaller than the repeat length of the polymer (30.1 Å). By assuming the most extended chain conformation, the tilt angle of polymer chain to the smectic layer normal was estimated as 41°. Thermodynamic data and inherent viscosity of the two polymers, PB-14-I and PB-14-II, are listed in Table 1.

**3.2. Stacked Lamellar Structure in the Smectic H Phase.** To perform SAXS measurements of the  $S_H$  liquid crystal, the sample was first heated to 260 °C and maintained at this temperature for about 5 min to

**Figure 2.** Temperature dependence of the  $d$  spacings of the inner and outer reflections observed for PB-14-I.

ensure isotropization. Then, it was cooled to the predetermined  $S_H$  temperature for the liquid crystallization at a rate of 160 °C min<sup>-1</sup>. After annealing for 20 min at that temperature, the sample was irradiated with X-ray for 40 min. Figure 3 shows the SAXS intensity profile of the  $S_H$  phase of PB-14-I prepared at 207 °C. Two scattering maxima with spacings of 200 and 133 Å can be easily observed. These were attributed to the second- and third-order reflections, although the first-order reflection with a spacing of 400 Å is significantly overlapped with the intense diffuse scattering from the central beam. The well-developed reflection profile thus shows that a stacked lamellar structure with a period of 400 Å exists in the  $S_H$  phase.

More insight into the lamellar structure was gained from electron micrographs of the ultrathin sections cut from the bulk sample. Figure 4 shows a typical electron microphotograph for the sample quenched from the  $S_H$  phase at 207 °C. The sections were stained with ruthenium tetroxide (RuO<sub>4</sub>), so the staining agent can be assumed to enter the disordered region. The bright parts, therefore, correspond to the lamellae separated by disordered regions which appear as the dark areas. The laterally large lamellae are formed with a thickness ranging from 300 Å to 400 Å, which roughly corresponds to that elucidated from the X-ray method. Furthermore, it is found that the disordered region is so narrow that the degree of liquid crystallinity is fairly high.

The stacked lamellar structure of the chain folding is common in linear polyesters, poly(ethylene terephthalate) and poly(butylene terephthalate). The present PB-14 polyester has a much longer flexible spacer than these, and so it is reasonable to conclude that it could accommodate the chain foldings in the smectic phase. The correlation length between foldings is approximate to the lamellar spacing of 400 Å, which corresponds to 13 times the length of the repeating unit.

**3.3. Dependence of Liquid Crystallization Temperature on Lamellar Thickness.** The lamellar sizes ( $L$ ) of the  $S_H$  phase for PB-14-I and PB-14-II were

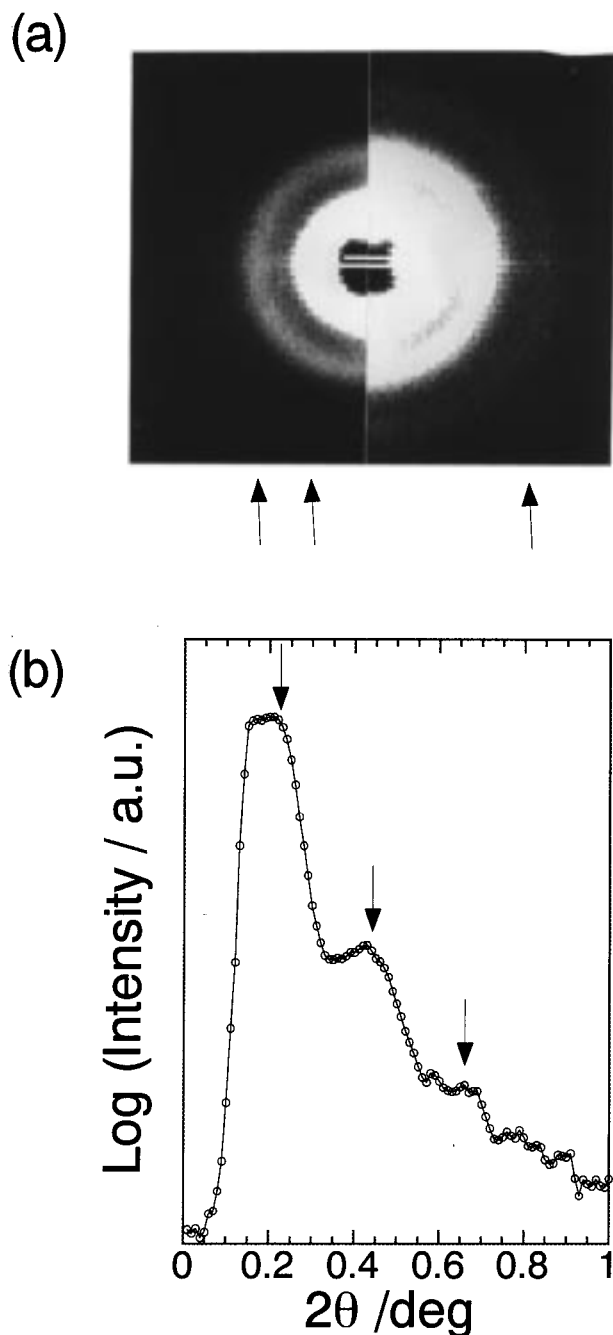


**Figure 3.** (a) Small-angle X-ray photograph and (b) the corresponding intensity profile recorded for the  $S_H$  phase of PB-14-I at 207 °C. The sample was quenched from the isotropic liquid state of 250 °C to the  $S_H$  phase of 207 °C. The arrows indicate the first, second, and third reflections.

collected at various liquid crystal temperatures as shown in Figure 5. Here, the lamellar sizes were determined from the second-order reflections in SAXS because the diffraction maxima greater than 350–400 Å cannot be resolved because of a significant overlapping with the central beam. Although the molecular weights are markedly different, the two specimens exhibited an identical dependence of the lamellar size on the liquid crystallization temperature. The lamellar spacing increases continuously with the liquid crystallization temperature. Similar dependence was also observed for the  $S_H$  phases of other PB- $n$  polyesters with  $n$  of 10–20.<sup>15</sup>

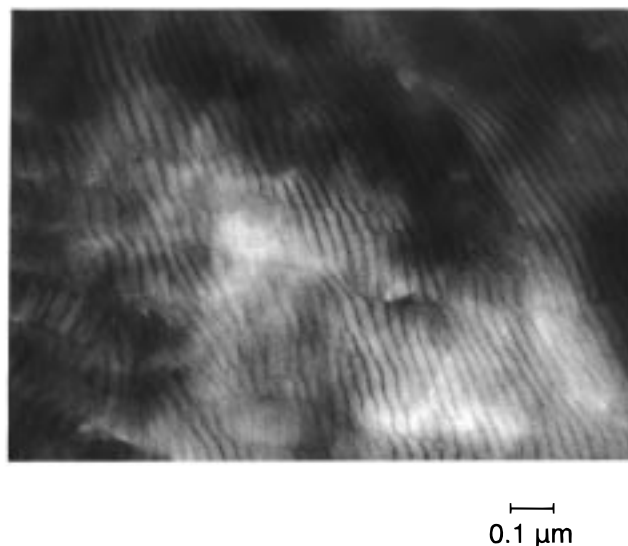


**Figure 4.** TEM photograph observed for the bulk PB-14-I specimen prepared by quenching the  $S_H$  phase of 207 °C.

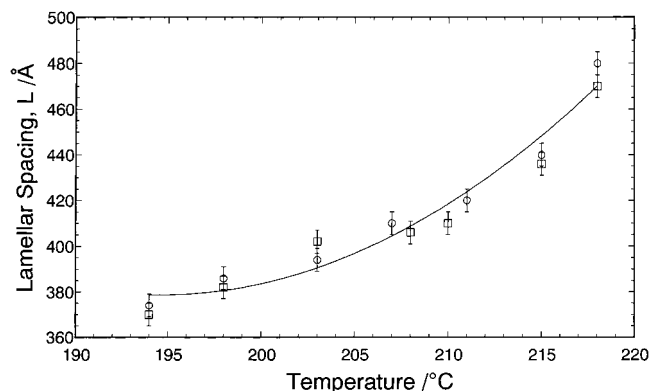


**Figure 5.** Dependence of the lamellar spacing on the liquid crystallization temperature observed for the  $S_H$  phases of PB-14-I (circle) and PB-14-II (square). The  $S_H$  sample was prepared by quenching from the isotropic liquid to the indicated temperature and annealed for 1 h. The lamellar spacings were determined from the second-order reflection of the SAXS measurements.

The DSC endotherms for the isotropization of the lamellar  $S_H$  liquid crystals were recorded with a Perkin-Elmer DSC II. Here, the  $S_H$  samples were prepared in DSC pan under the same condition of liquid crystallization as in the SAXS measurements, and heated to isotropization at a rate of 10 °C min<sup>-1</sup>. The isotropization temperatures ( $T_i$ ) are presented in Figure 6 as a function of reciprocal lamellar spacing ( $1/L$ ) determined by the SAXS measurements. The data are consistent with a straight line and the relationship between  $T_i$  and  $L$  are described by the equation

$$T_i \text{ (K)} = T_i^\circ (1 - a/L) \quad (1)$$

which corresponds to the Thomson–Gibbs equation expected for a lamellar crystallite of large lateral dimensions and finite thickness.<sup>7,16,17</sup> The data extrapolates to  $T_i^\circ$  of 536 K (263 °C), which can be regarded as the isotropization temperature of the  $S_H$  liquid crystal with an infinite lamellar thickness.<sup>17</sup> The value of  $a$  ( $= 2\sigma_e/\Delta h_f$ ) is 22.0 Å, where  $\Delta h_f$  is the bulk heat of fusion and  $\sigma_e$  is the top and bottom specific surface free energy. By putting the values of  $\Delta h_f = 6.0 \text{ kcal mol}^{-1}$  and the lattice volume  $v_o = 6.1 \times 9.0 \times 22.7 \text{ Å}^3$  (two repeat

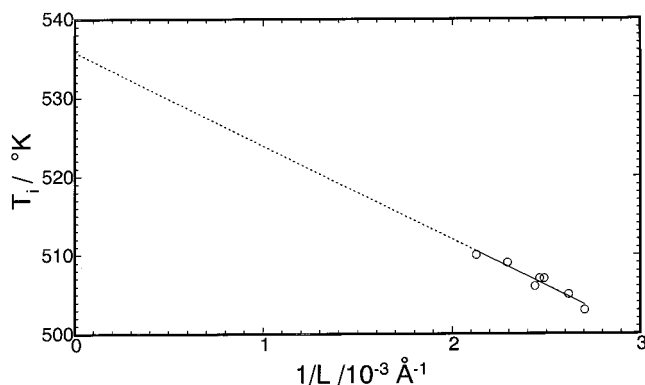


**Figure 6.** Isotropization temperatures for the  $S_H$  phase of PB-14-I as a function of reciprocal lamellar spacing.

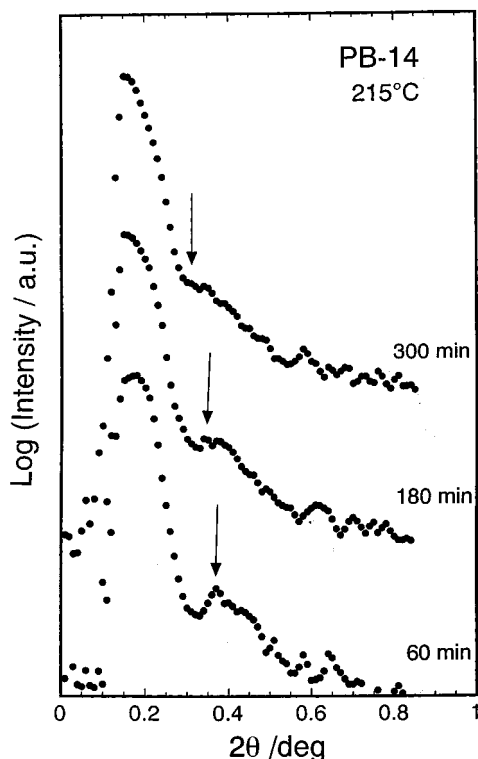


**Figure 7.** SAXS intensity profiles recorded for the  $S_H$  phase of PB-14-II annealed at 215 °C for the different time periods given in the figure. The arrows indicate the second-order reflection.

units) $^{-1}$ , we could calculate 72 erg  $\text{cm}^{-2}$  for the value of  $\sigma_e$ . This value is similar to 87 erg  $\text{cm}^{-2}$  in the polyethylene lamellar crystal.<sup>16</sup>

**3.4. Thickening of Lamellae by Annealing.** Figure 7 illustrates the SAXS intensity profiles for the samples annealed for different periods at a  $S_H$  temperature of 215 °C. The second-order scattering peak shifted to a smaller angle, simultaneously becoming broad with an increase in the annealing period, and was overlapped with the strong scattering around the central beam. Although it is obvious that lamellar thickening takes place, the accurate lamellar sizes could not be determined from the SAXS measurement. We therefore speculated upon the lamellar size from  $T_i$  by using the eq 1 as follows.

Figure 8 shows the DSC endotherms for the isotropization of the  $S_H$  samples of PB-14-II annealed at 215 °C for the times indicated. To obtain the DSC endotherms with a certain baseline, the sample was first

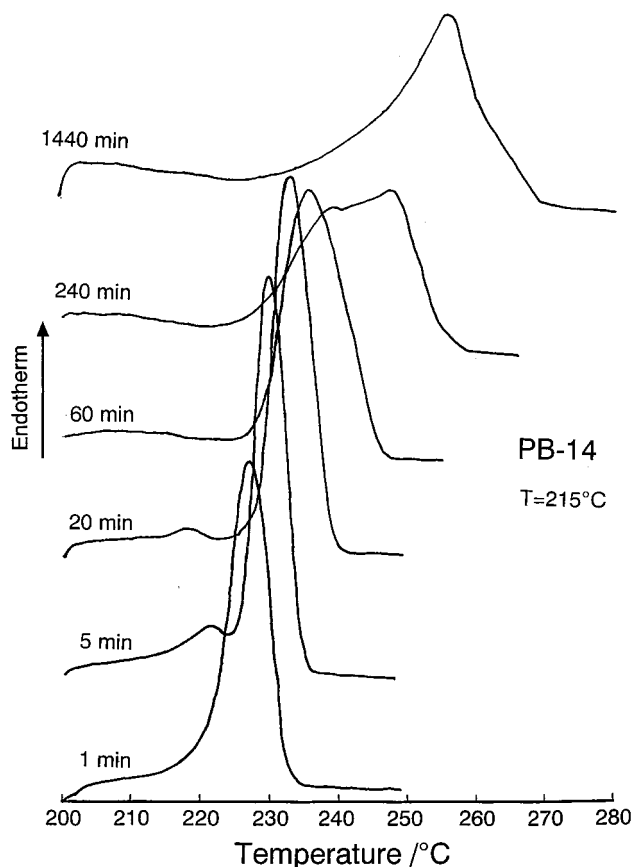


**Figure 8.** DSC endotherms obtained on isotropization for the  $S_H$  phase of PB-14-II at a scanning rate of 10 °C  $\text{min}^{-1}$  after annealing at 215 °C for various times indicated in the figure.

cooled rapidly from 215 °C to 200 °C, and then heated to the isotropization at a rate of 10 °C  $\text{min}^{-1}$ . The shape and temperature of the endothermic peak significantly depended on the annealing time. The sample annealed for 1 min showed a single peak at 228 °C. On increasing the annealing time, the endothermic peak position shifted to a higher temperature, and a small peak appeared at a lower temperature although it disappeared after 60 min. The main peak becomes broadened and separated into two peaks after 240 min. After annealing for 1440 min (24 h), a single broad peak appeared at 257 °C. Because all the annealed samples exhibited the same cooling and heating DSC thermograms as in Figure 1 once they experienced the isotropic melt, the shift of  $T_i$  by annealing is attributed to the lamellar thickening, but not to polymerization or decomposition. In Figure 9, the lamellar spacings calculated from  $T_i$  by using the eq 1 are plotted (shown in circles) against the annealing time. The lamellar spacing increases from 330 to 2000 Å. Simultaneously, the isotropization enthalpy increases from 4.9 to 6.0 kcal  $\text{mol}^{-1}$  as shown by rectangles in Figure 9, reflecting the increase of liquid crystallinity. Thus the degree of liquid crystallinity increases with the lamellar thickening, which corresponds to a decrease of the probability of the folding sites. The folding sites may not be accommodated into the  $S_H$  structure, because the mesogens in the  $S_H$  phase should adopt a monoclinic layer packing.

Chain folding in the  $S_H$  phase may arise from a kinetic factor as generally discussed for the crystallization of conventional polymers. In the  $S_H$  phase, a rapid exchange between trans and gauche conformations of the alkyl spacer takes place and the two phenyl rings in



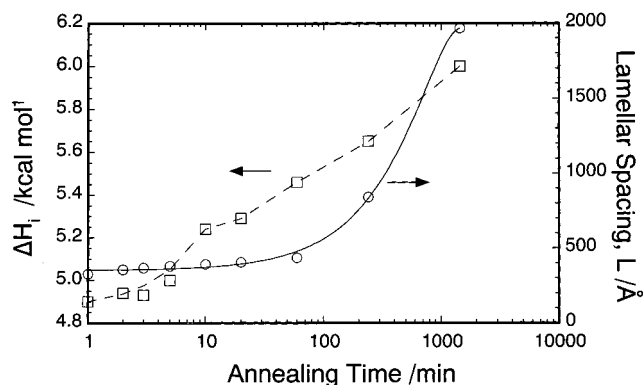


**Figure 9.** Annealing time dependence of the lamellar size (circle) and isotropization enthalpy (square) for the  $S_H$  phases of PB-14-II annealed at 215 °C. Here, the lamellar size was estimated from the isotropization temperature by using the eq 1.

the mesogenic moiety rotate around the central bond within a limited angle according to the analysis of solid-state  $^{13}\text{C}$  NMR spectra,<sup>14</sup> suggesting that the polymer chain is mobile in the  $S_H$  phase. Lamellar thickening in the  $S_H$  state may result from the conformational change from a folded to an extended form that is more suitable for the monoclinic packing of mesogens.

#### 4. Concluding Remarks

The LC state morphology was studied for the main-chain LC polyester, PB-14, which forms the  $S_H$  phase. The well-defined lamellar structure was detected in the  $S_H$  phase from SAXS and electron microscopic measurements. The lamellar spacing increased with an increase in the liquid crystallization temperature, and the isotropization temperature of the  $S_H$  phase depended on the lamellar size as described with a variant of the Thomson–Gibbs equation. The top and bottom surface free energy of the lamellae was elucidated as 72 erg cm<sup>-2</sup>.

By annealing at a  $S_H$  temperature of 215 °C, the isotropization temperature of the  $S_H$  phase increased from 228 °C to 257 °C. According to the Thomson–Gibbs equation, the increase in  $T_i$  corresponds to an increase in the lamellar size from 300 to 2000 Å. The isotropization enthalpy of the  $S_H$  phase also increased from 4.9 kcal mol<sup>-1</sup> to 6.0 kcal mol<sup>-1</sup>. Transformation from isotropic melt to the  $S_H$  mesophase thus takes place imperfectly in a finite period due to chain folding

raised from a kinetic factor. Furthermore, the lamellar thickening may be followed by an alteration in the polymer chain conformation from a folded to an extended form that is suitable for the  $S_H$  liquid crystal structure. The whole feature of the liquid crystallization of the  $S_H$  phase is thus similar to that of the crystallization observed for conventional polymers, but different from that of the liquid crystallization of the  $S_A$  phase.<sup>6,7</sup> This may be due to the highly ordered structure of the  $S_H$  phase so that the folding sites are not compatible with the ordered  $S_H$  structure and form the boundary of lamellae.

**Acknowledgment.** One of the authors (M. T.) wishes to express sincere thanks to Professors Seizo Miyata and Toshiyuki Watanabe of Tokyo University of Agriculture and Technology for helpful discussions and encouragement.

#### References and Notes

- (1) Watanabe, J.; Hayashi, M.; Nakata, Y.; Niori, T.; Tokita, M. *Prog. Polym. Sci.* **1997**, *22*, 1053.
- (2) de Gennes, P. G. In *Polymer Liquid Crystals*; Cifferri, A.; Krigbaum, W. R.; Mayer, R. B., Eds.; Academic Press: New York, 1982; p 124.
- (3) Williams, D. R. M.; Warner, M. *J. Phys. Fr.* **1990**, *51*, 317.
- (4) Li, M. H.; Brulet, A.; Davidson, P.; Keller, P.; Cotton, J. P. *Phys. Rev. Lett.* **1993**, *70*, 2293.
- (5) Li, M. H.; Brulet, A.; Cotton, J. P.; Davidson, P.; Strazielle, C.; Keller, P. *J. Phys. II (France)* **1994**, *4*, 1843.
- (6) Tokita, M.; Takahashi, T.; Hayashi, M.; Inomata, K.; Watanabe, J. *Macromolecules* **1996**, *29*, 1345.
- (7) Tokita, M.; Osada, K.; Watanabe, J. *Liq. Cryst.* **1997**, *23*, 453.
- (8) Krigbaum, W. R.; Watanabe, J. *Polymer* **1983**, *24*, 1299.
- (9) Tokita, M.; Osada, K.; Kawauchi, S.; Watanabe, J. *Polym. J.* **1998**, *30*, 687.
- (10) Krigbaum, W. R.; Watanabe, J.; Ishikawa, T. *Macromolecules* **1983**, *16*, 6, 1271.
- (11) Watanabe, J.; Krigbaum, W. R. *Macromolecules* **1984**, *17*, 2288.
- (12) Maeda, Y.; Mabuchi, T.; Watanabe, J. *Thermochim. Acta* **1995**, *266*, 189.
- (13) Huang, H. W.; Horie, K.; Yamashita, T.; Machida, S.; Sone, M.; Tokita, M.; Watanabe, J.; Maeda, Y. *Macromolecules* **1996**, *29*, 3485.
- (14) Tokita, M.; Sone, M.; Kurosu, H.; Ando, I.; Watanabe, J. *J. Mol. Struct.* **1998**, *446*, 215.
- (15) Osada, K.; Tokita, M.; Watanabe, J. to be published.
- (16) Wunderlich, B. *Macromolecular Physics*; Academic Press: New York, 1980.
- (17) Lu, L.; Alamo, R. G.; Mandelkern, L. *Macromolecules* **1994**, *27*, 6571.

MA9810161